

# Simple Model of Capillary Condensation in porous media.

S. M. Gatica<sup>1</sup>, M. M. Calbi<sup>2</sup> and M. W. Cole<sup>2</sup>

<sup>1</sup>*Departamento de Física, Facultad de Ciencias Exactas  
y Naturales, Universidad de Buenos Aires, 1428 Buenos Aires  
Argentina*

<sup>2</sup>*Department of Physics, The Pennsylvania State University,  
University Park, Pennsylvania 16802*

(November 2, 2018)

## Abstract

We employ a simple model to describe the phase behavior of <sup>4</sup>He and Ar in a hypothetical porous material consisting of a regular array of infinitely long, solid, parallel cylinders. We find that high porosity geometries exhibit two transitions: from vapor to film and from film to capillary condensed liquid. At low porosity, the film is replaced by a “necking” configuration, and for a range of intermediate porosity there are three transitions: from vapor to film, from film to necking and from necking to a capillary condensed phase.

## I. INTRODUCTION

The physics of adsorption in porous media has long been appreciated for its considerable importance in diverse applications, including gas storage, separations and cryopumping. In addition, the geometry provokes intriguing fundamental questions about the properties of phases of the adsorbate, for which the surface curvature energy plays a prominent role [1–7]. An ongoing question pertains to the validity of numerous simple quasi-two or one dimensional models which omit the heterogeneity present in most such media. [8,9] Moreover, there remains a fundamental question about the nature and existence of genuine phase transitions in such disordered media.

In this paper, we attempt to answer *qualitative* questions about the nature of such adsorption by employing a simple model of the geometry that we study with a simple calculational procedure. The geometry is shown in figure 1 and described in detail below. The procedure is called a “simple model” in a number of papers published over the last decade [10–17]. In the model, the system’s energy is taken as a straightforward sum of bulk energy, surface energy and gas-solid interaction energy terms. The model is certainly oversimplified; yet it has provided answers to questions about similar adsorption problems which agree rather well with results obtained in more reliable (even “exact”) studies of the same problem. The rationale for applying the present approach is that the results may yield broad trends which

are robust, at least qualitatively. In the present case, our results are phase diagrams for which a key parameter is the porosity  $\Phi$  of the system. As expected, the physics of pore filling involves a competition between adhesive and cohesive forces. As such, the results of our calculations are sensitive to assumptions we make about the gas-surface interaction. In the present case, both these assumptions and the calculational results are analogous to those found in the problem of wetting transitions. [18]

## II. THE MODEL

We propose a simple model consisting of infinitely long, solid, parallel cylinders of radius  $R = 30\text{\AA}$ . The centers of the cylinders form a square lattice and the distance between sites,  $S$ , is related to  $\Phi$  by the equation

$$\Phi = 1 - \frac{\pi R^2}{S^2}. \quad (1)$$

The configuration is depicted in Fig. 1, where is also shown the triangular unit cell considered in the calculations. The interaction between the adsorbed atoms and the substrate is approximated by the sum of the potentials from the four cylinders that are closest to the unit cell. The potential due to each single cylinder,  $V$ , was constructed assuming cylindrical symmetry so that it is a function of the distance to the axis only ( $r$ ). The following function  $V(r)$  reproduces both the potential of a flat substrate (which has often been modeled as  $4C_3^3/(27D^2z^9) - C_3/z^3$ ,  $z$  being the distance from the surface) for  $r \rightarrow R$  and the potential of an infinite wire for  $r \gg R$ ,

$$V(r) = \frac{4C_3^3}{27D^2} \frac{1}{(r-R)^9} - \frac{C}{(C/C_3 - R^2 + r^2)(r-R)^3}, \quad (2)$$

where  $D$  and  $C_3$  are the well depth and van der Waals parameters respectively [19,20] and  $C = 9\frac{\pi}{4}C_3R^2$ . We adopted values displayed in table I that are intermediate between the strongly attractive graphite and the weakly attractive alkali metals. The form of  $V(r)$  and the total interaction considering four cylinders are plotted in Fig. 2.

Atoms adsorbed in this material below saturated vapor pressure are expected to form either a film adsorbed on the wall of the substrate, or a condensed phase (C) filling all the free space. Which of the two phases is stable can be determined by evaluating and comparing the free energies. If the film is stable, and the porosity is moderately low (<50%), the fluid may form bridges or “necks” between neighboring cylinders (see Fig. 3). We will refer to this configuration as “necking” (N), and apply the term “film” (F) to the case where no necks are formed. The letter E refers to the empty pore configuration. This actually means the presence of a low density vapor phase, which is “empty” only by contrast to the higher density liquid phase.

For a given value of the chemical potential  $\mu$  below saturation ( $\mu_0$ ), we evaluate the grand free energy per unit length

$$\Omega = F/L - \mu N/L. \quad (3)$$

$F$  is the Helmholtz free energy, consisting of the substrate-fluid interaction, a bulk free energy and the surface energy. Assuming translational symmetry along the coordinate parallel to

the axis of the cylinders,  $z$ , the grand free energy per unit length of the fluid contained in the unit cell is, for the phase C

$$\Omega_C = n \int_0^{\pi/4} d\phi \int_{r_{min}}^{S/(2\cos(\phi))} V(r)rdr - n(\mu - \mu_0)(S^2 - \pi r_{min}^2)/8 + \sigma \frac{\pi}{4} r_{min}. \quad (4)$$

Here  $\sigma$  and  $n$  are the bulk surface tension and number density of the fluid at a given temperature, and  $r_{min}$  is a cutoff distance, chosen as the radius where the potential due to a single cylinder is minimum. We are taking the surface tension for the solid-liquid interface to consist of the sum of the liquid-vapor interfacial tension and the integrated solid-fluid potential energy. In this model, we are assuming that a fluid of density  $n$  fills all the available space homogeneously, except the region  $r < r_{min}$ . For the phase F we consider a homogeneous film of density  $n$  formed between  $r_{min}$  and  $r_e(\phi)$ , the energy reads

$$\Omega_F = n \int_0^{\pi/4} d\phi \int_{r_{min}}^{r_e(\phi)} V(r)rdr + \sigma \int_{\phi_N}^{\pi/4} d\phi \sqrt{r_e(\phi)^2 + r_e'(\phi)^2} - \frac{1}{2}n(\mu - \mu_0) \int_0^{\pi/4} d\phi (r_e(\phi)^2 - r_{min}^2) + \sigma \frac{\pi}{4} r_{min}, \quad (5)$$

where  $r_e(\phi)$  is the equilibrium profile, and  $\phi_N$  is the angle subtended by the neck (see Fig. 3) if present, taken to be zero for a film. A prime in this expression means a derivative with respect to  $\phi$ .

By minimizing the energy  $\Omega_F$ , we get a differential equation for  $r_e(\phi)$ :

$$\mu - \mu_0 - V[r_e(\phi)] = \frac{\sigma}{nR[r_e(\phi)]}, \quad (6)$$

where  $R[r_e(\phi)]$  is the radius of curvature,

$$R[r(\phi)] = \frac{(r(\phi)^2 + r'(\phi)^2)^{3/2}}{2r'(\phi)^2 + r(\phi)(r(\phi) - r''(\phi))} \quad (7)$$

Notice that if the surface tension is small the right hand side of eq. 6 can be neglected and the following condition results

$$V[r_e(\phi)] = \mu - \mu_0. \quad (8)$$

This is the equation for the equipotential curves; its use corresponds to the venerable Polanyi theory of adsorption [21]. In the present study, we use this relation, instead of solving eq.6, because it greatly simplifies the calculation. The approximation is good in a range of chemical potential such that

$$\mu_0 - \mu \gg | \sigma/nR[r_e(\phi)] | \quad (9)$$

for all  $\phi$ . It will be shown below that in the case of He, the relevant values of  $\mu$ , where we find phase transitions, fulfill this condition. For Ar, that is not the case at temperatures close to the triple point (i.e., when the surface tension is maximum). These behaviors will be discussed in the next section.

### III. RESULTS

In Fig. 4 a) we display the grand free energy of the phases F and C for Ar at  $T = 130K$  and porosity  $\Phi = 0.42$ , which corresponds to a separation  $d = 10\text{\AA}$  between the cylinders. Observe that  $\Omega_C$  and  $\Omega_F > 0$  for  $\delta\mu^* = (\mu - \mu_0)/\epsilon < -1.7$ ; hence the empty phase is stable in this regime. However  $\Omega_F < \Omega_C$  and  $\Omega_F < 0$  for  $-1.7 < \delta\mu^* < -0.28$ , so the film is stable there, while for  $\delta\mu^* > -0.28$  the completely filled phase is stable. In Fig. 4 b) we plot the corresponding isotherm, together with the derivative  $dN/d\mu$ . The steps in the isotherm correspond to the transitions E $\rightarrow$ F and N $\rightarrow$ C, and the peak in  $dN/d\mu$  corresponds to the transition F $\rightarrow$ N. From similar analysis for different porosities, we construct the phase diagram shown in Fig. 5. The line of the phase diagram is dotted in the region where the condition given by eq. 9 fails, according to the following criterion: in the case of films the quantity  $\sigma/nR[r_e]$  will be smaller than  $\sigma/nr_{min} \equiv -\delta\mu_{min}^*$ , so we consider that the condition (9) is fulfilled if  $\delta\mu^* < 10 \delta\mu_{min}^*$ . In the case of necking, the curvature radius for  $\phi \simeq \phi_N$  is not necessarily larger than  $r_{min}$  and therefore  $r_{eq}(\phi \sim \phi_N)$  is poorly determined. However, the error introduced to the energy by this difference in the profile is expected to be small. For temperatures closer to the triple point, the surface tension (and therefore  $-\delta\mu_{min}^*$ ) is larger, and the transitions occur at values of  $\mu$  such that  $\delta\mu^* > 10 \delta\mu_{min}^*$ , so the analysis done using eq. 8 becomes meaningless for such low temperatures. As is seen in Fig. 5, the phase N is possible only for very low porosities (small  $d$ ), where the volume-filling “price” of necking is smaller. The upper part of the diagram is qualitatively equivalent to the one obtained for a slab with large separation between walls. (see Fig.4 in ref. [10])

The corresponding energies calculated for He are shown in Fig. 6 for two different temperatures and  $\Phi = 0.42$ , together with the components of  $\Omega_F$ , on the right. By means of the same procedure described above for Ar, we derived the phase diagrams displayed in fig. 7. The scenario is the same as for Ar. Comparing the results for  $T = 0$  K and 3 K, we notice that at higher temperature there is a wider region where F is stable. This can be explained in terms of the values of the surface tension: for  $T=3$  K,  $\sigma/n$  is 30% smaller than for  $T=0$  K. This is evident in Fig. 6, on the right, where we can see that the contribution of the surface energy to  $\Omega_F$  is more important for  $T=0$  K than for 3 K. As a consequence, the phase F, that requires the formation of an interface, is more favorable at higher temperatures. For Ar, the region of the phase diagram corresponding to the phase F is even narrower, as is expected since the surface energy relative to the substrate potential energy (in relative terms) is larger for Ar than for He at any temperature.

### IV. COMMENTS

In this paper we have derived the phase behavior for gases exposed to an array of parallel cylindrical strands of material. Using a number of simplifying assumptions, this calculation yields a kind of generic behavior, exemplified by the similarity of the behavior predicted for a classical fluid (Ar) and an extreme quantum fluid ( $^4\text{He}$ ). The behavior is such that low porosity ( $\Phi < 0.4$ ) geometries exhibit a necking transition at low chemical potential, followed by capillary condensation. For a narrow range of intermediate porosity ( $0.4 < \Phi < 0.5$ ), the behavior is different: a thin film forms, followed by necking (with a singular derivative but no discontinuity in the isotherm), followed by capillary condensation. At porosity  $\Phi > 0.5$ ,

there is a transition from film to capillary condensation and necking does not occur at any chemical potential. We note that the Kelvin equation does not agree with the present results for the threshold of capillary condensation. This discrepancy is well known from similar studies of small pores, due to the equation's neglect of the substrate potential and the resulting depleted density region near the wall (so that the pore radius is ill-defined). [22]

This research has been funded in part by the Army Research Office, the Petroleum Research Fund, the American Chemical Society, CONICET and the University of Buenos Aires.

## TABLES

TABLE I. Well depth and van der Waals coefficients  $D$  and  $C_3$  used in the calculation and parameters of the gas-gas interaction,  $\epsilon$  and  $\sigma$  from ref. [23].

	$\epsilon(meV)$	$\sigma(\text{\AA})$	$D(meV)$	$C_3(meV\text{\AA}^3)$
Ar	10.34	3.40	50	1000
He	0.88	2.56	7	150

FIGURES

FIG. 1. Schematic diagram of the configuration; the unit cell is shown with dashed lines.

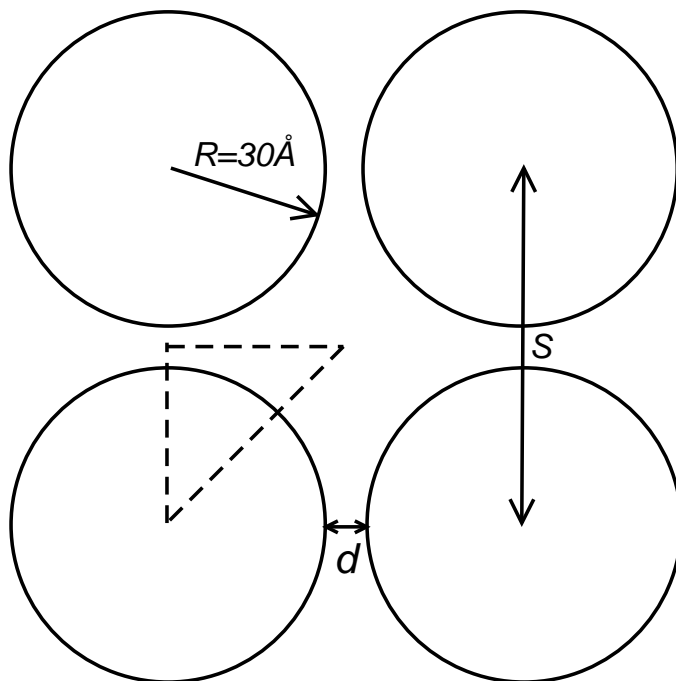


FIG. 2. a) Equipotential curves due to the four closest cylinders (with  $\Phi = 0.42$ ), for He. Contours are labelled by potential energy values, in meV. The dashed line shows a boundary of the unit cell. b) Potential contributed by a single cylinder for He (dashed) and Ar (solid).

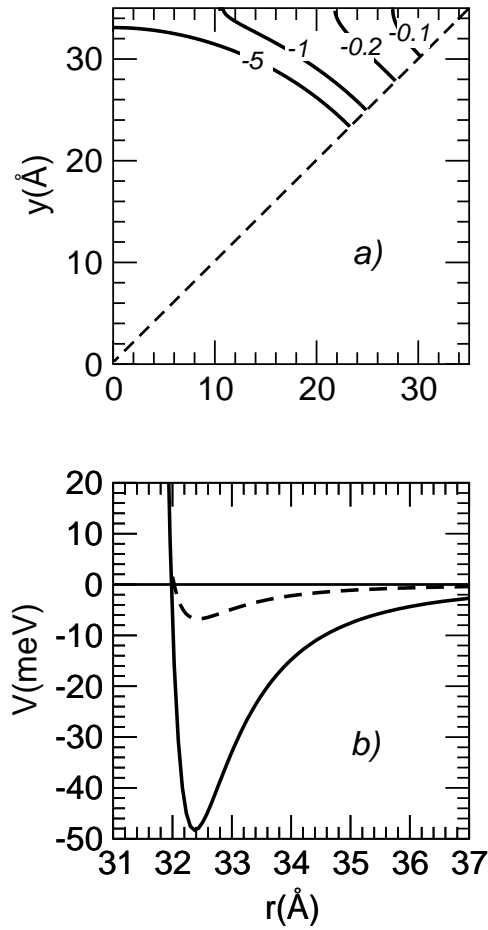




FIG. 3. Schematic views of the film phase (left) and necking phase (right).

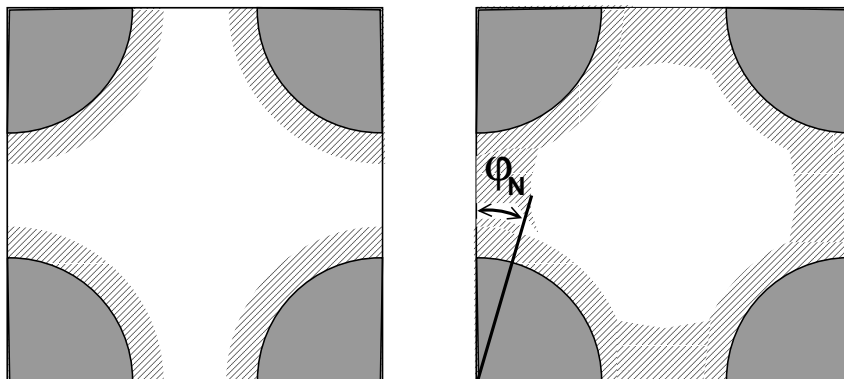


FIG. 4. a) Grand free energies for Ar at  $T = 130K$  ( $\Phi = 0.42$ ). b) Number of atoms per unit length (solid line) and  $dN/d\mu$  (dashed line, in arbitrary units). The vertical line at the isotherm step corresponds to a delta function in this derivative.

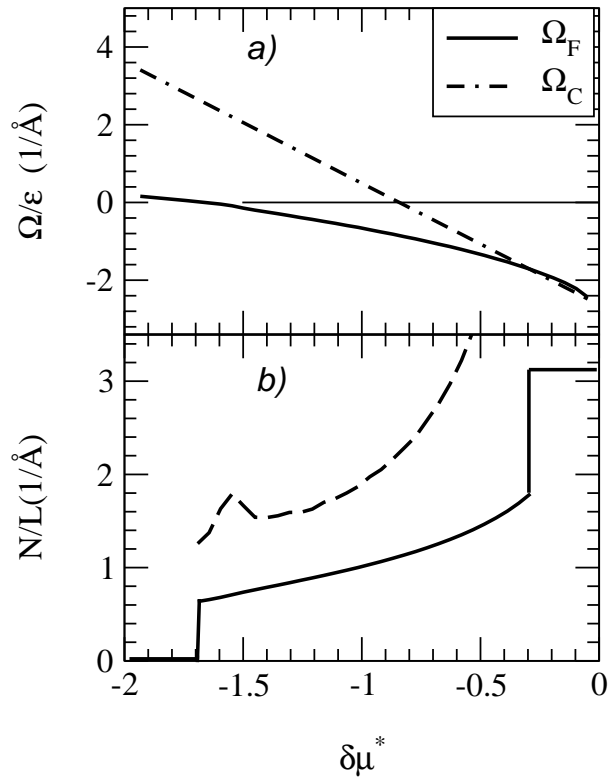


FIG. 5. Phase Diagram for Ar at  $T = 130K$ . The dotted portion of the curves are explained in the text.

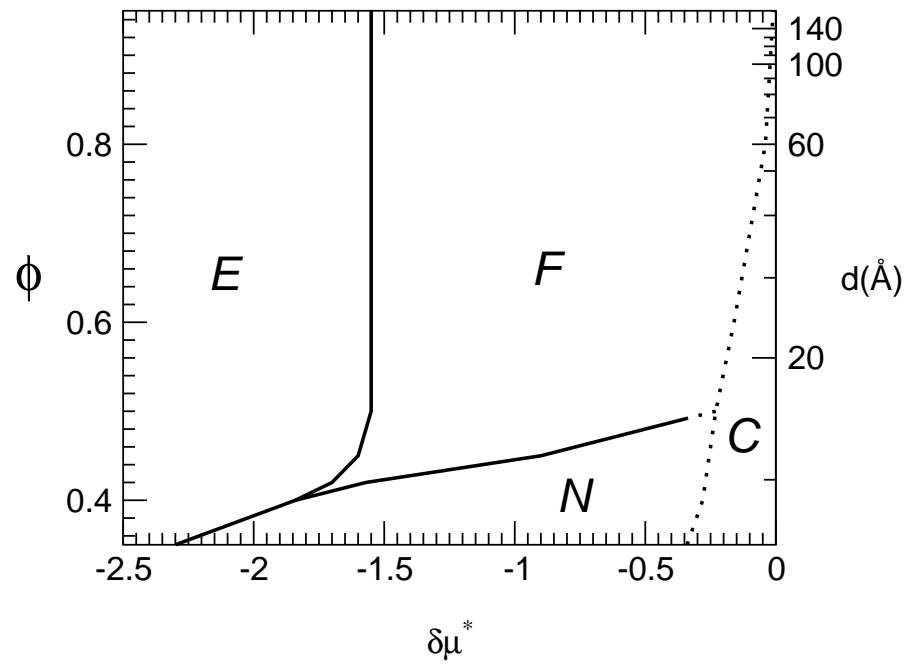


FIG. 6. Pore-filling behavior for helium at  $T=0$  and  $3K$ . Left panels show the grand free energies  $\Omega_F$  (solid line) and  $\Omega_C$  (dashed line) for He at the temperature indicated. Right panels show the energy contributions to  $\Omega_F$ , due to the surface (dotted line), substrate (dashed line) and volume (dotted-dashed line).

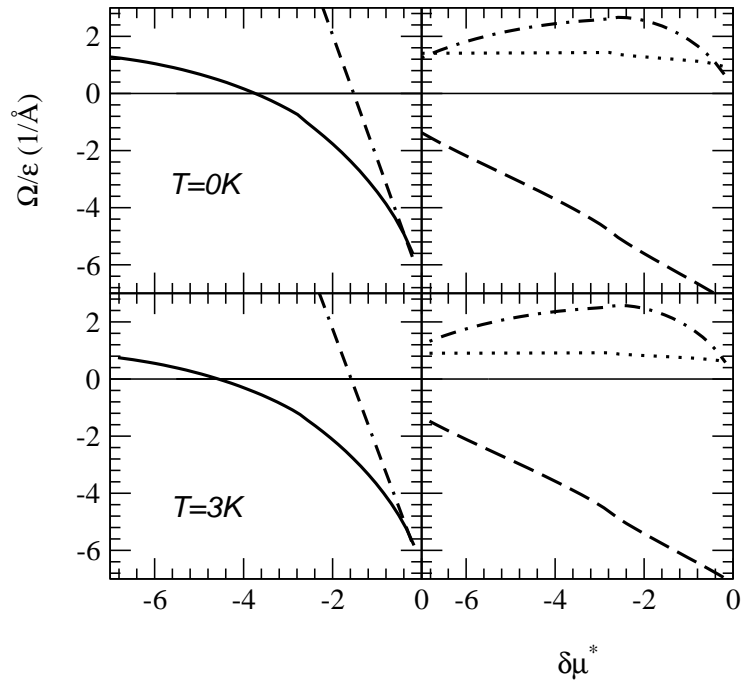
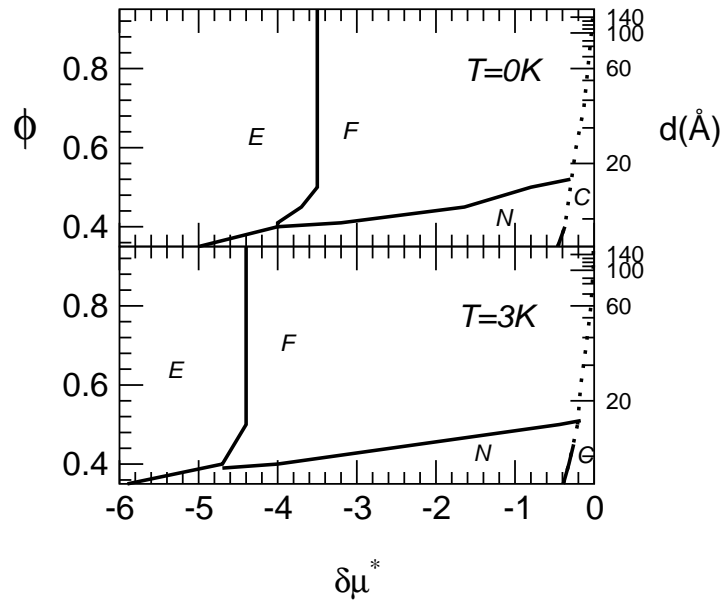


FIG. 7. Phase Diagram for He, at the temperatures indicated.



## REFERENCES

- [1] Lev D. Gelb, K. E. Gubbins, R. Radhakrishnan and M. Sliwinska-Bartkowiak, Rep. Prog. Phys. **62** (1999) 1573-1659.
- [2] A. P. Y. Wong and M. H. W. Chan, Phys. Rev. Lett. **65**, 2567 (1990).
- [3] A. P. Y. Wong, S. B. Kim, W. I. Goldburg and M. H. W. Chan, Phys. Rev. Lett. **70**, 954 (1993).
- [4] M. Thommes, G. H. Findenegg, Langmuir **10**, 4270 (1994).
- [5] M. Schoen, *Computer simulation of condensed phases in complex geometries* (Springer-Verlag, Berlin, 1993).
- [6] S. Dietrich and M. L. Rosinberg, in *New Approaches to Problems in Liquid State Theory*, C. Caccamo et al. (Eds.) (Kluwer, Dordrecht, 1999).
- [7] R. Evans, in *Fundamentals of Inhomogeneous Fluids*, D. Henderson (Ed.) (Marcel Dekker, New York, 1992).
- [8] K. S. Page and P. A. Monson, Phys. Rev. E. **54**, 6557 (1996).
- [9] M. Miyahara, K. E. Gubbins, J. Chem. Phys. **106**, 2865 (1997).
- [10] S. M. Gatica, M. Calbi and M. W. Cole, Phys. Rev. E **59**, 4484 (1999).
- [11] M. M. Calbi, F. Toigo, S. M. Gatica and M. W. Cole, Phys. Rev. B **60**, 14935 (1999)
- [12] F. Ancilotto and F. Toigo, Phys. Rev. B **60**, 9019 (1999).
- [13] M. J. Bojan, G. Stan, S. Curtarolo, W. A. Steele, and M.W. Cole, Phys. Rev. E **59**, 864 (1999).
- [14] G. Mistura, F. Ancilotto, L. Bruschi, and F. Toigo, Phys. Rev. Lett. **82**, 795 (1999).
- [15] F. Ancilotto, F. Faccin, and F. Toigo, Phys. Rev. **62**, 17 035 (2000).
- [16] E. Cheng, M. W. Cole, W. F. Saam and J. Treiner, Phys. Rev. B **48**, 18214 (1993).
- [17] S. Curtarolo, G. Stan, M. J. Bojan, M. W. Cole, and W. A. Steele, E **61**, 1670 (2000).
- [18] D. Bonn and D. Ross, Rep. Prog. Phys. **64** (2001) 1085-1163.
- [19] A. Chizmeshya, M. W. Cole, and E. Zaremba, J. Low Temp. Phys. **110**, 677-684 (1998).
- [20] G. Vidali, G. Ihm, H. Y. Kim and M. W. Cole, Surface Science Reports **12**, 133-182 (1991)
- [21] M. Polanyi, Trans. Far. Soc. **28**, 316 (1932)
- [22] R. Evans, *Liquids at Interfaces*, ed. J. Charvolin, J.F. Joanny, J.Zinn-Justin (Elsevier, Amsterdam, 1990).
- [23] R. O. Watts and I. J. McGee, *Liquid State Chemical Physics* (Wiley, New York, 1976).